

Spectroscopy and flavor changing decays of B , B_s mesons in a Dirac formalism

Manan Shah,^{1,*} Bhavin Patel,^{1,†} and P. C. Vinodkumar^{2,‡}

¹*P. D. Patel Institute of Applied Sciences, Charusat, Changa 388 421, India*

²*Department of Physics, Sardar Patel University, Vallabh Vidyanagar 388 120, India*

(Received 20 February 2016; published 25 May 2016)

In the framework of the relativistic independent quark model, the mass spectra and decay properties of B and B_s mesons are obtained using a Martin-like potential for the quark confinement. The predicted excited states are in good agreement with the experimental results as well as with the lattice QCD and other theoretical predictions. For instance, the $B_2(5747)$ as 1^3P_2 , $B_1(5721)$ as 1^3P_1 , and $B_0(5732)$ as 1^3P_0 are identified. The spectroscopic parameters are used to calculate the electromagnetic transitions, pseudoscalar decay constants, hadronic decay widths, and leptonic decay widths. The present result for the decay constant, $f_B(1S) = 188.56$ MeV, is in good agreement with recent lattice results (UKQCD Collaboration, Fermilab) and comparable with the experimental value of (206.7 ± 8.9) . The pseudoscalar decay constant for the B_s meson obtained here, $f_{B_s}(1S) = 240.21$ MeV, is in very good agreement with recent lattice QCD and QCD sum rule predictions. The predicted branching ratio for $B^+ \rightarrow \tau^+ \nu_\tau$ (1.354×10^{-4}) is in accordance with the value, $(1.65 \pm 0.34) \times 10^{-4}$ reported by the Particle Data Group (PDG). The branching ratios of the rare decays $B_s^0 \rightarrow \mu^+ \mu^-$ ($(3.1 \pm 0.7) \times 10^{-9}$) and $B^0 \rightarrow \mu^+ \mu^-$ ($< 6.3 \times 10^{-10}$) as observed by the CMS and LHCb Collaborations very recently are in accordance with our predictions of 3.602×10^{-9} and 1.018×10^{-10} , respectively. The Cabibbo-favored hadronic branching ratios of $B^0 \rightarrow D^- \pi^+$ (3.724×10^{-3}), $B^0 \rightarrow D^{*-} \pi^+$ (3.475×10^{-3}), and $B_s \rightarrow D_s^- \rho^+$ (3.800×10^{-3}) are in good agreement with the respective PDG values. The mixing parameters x_q, χ_q for $B^0 - \bar{B}^0$ ($x_d = 0.769$, $\chi_d = 0.1859$) and $B_s - \bar{B}_s$ ($x_s = 26.41$, $\chi_s = 0.49929$) are also found to be in excellent agreement with the PDG values of $(0.770 \pm 0.008, 0.1862 \pm 0.0023)$ and $(26.49 \pm 0.29, 0.499292 \pm 0.000016)$, respectively.

DOI: [10.1103/PhysRevD.93.094028](https://doi.org/10.1103/PhysRevD.93.094028)

I. INTRODUCTION

Recent observations of various hadronic states (particularly in the heavy-flavor sector) by different experimental groups have revitalized the field of hadron spectroscopy [1,2]. Though a large number of these newly observed states are in the charm sector, there are many newly observed states in the beauty (bottom) sector as well. It has generated a vast interest in the heavy-flavor sector. For instance, the masses of low-lying $1S$ and $1P_J$ states of B and B_s mesons were recorded experimentally [1] and many of their excited states were predicted theoretically [3–11]. Experiments at CDF and DØ found several narrow B and B_s states, such as $B_1(5720)$, $B_2^*(5745)$, and $B_{s2}^*(5839)$ [12]. Among the various experimentally observed B and B_s meson states [B^* , B , $B_2(5747)$, $B_1(5721)$, $B_0(5732)$, B_s^* , B_s , $B_{s2}(5840)$, $B_{s1}(5830)$, $B_{s1}(5850)$], many of the predicted states are missing. For example, there is no evidence for $2S$, $1D$ states of B and B_s mesons and the center of mass of the $1P$ state. These unconfirmed states of B and B_s mesons have further generated considerable

interest towards the spectroscopy of doubly open flavor mesons. The CDF Collaboration has very recently announced evidence of a new resonance $B(5970)^{+/-0}$ in the $B^0 \pi^+ / B^+ \pi^-$ invariant mass spectrum [13]. This state $B(5970)$ was also predicted theoretically [14] through the effective Lagrangian approach. They have assigned it as the 2^3S_1 state in the B meson family, while heavy meson effective theory [15] predicted this bottom meson as either the $2S(1^-)$, $1D(1^-)$, or $1D(3^-)$ state. Thus, recent experimental data on excited B and B_s states are partially inconclusive and require more detailed analysis involving their decay properties. In this context, we focus on only the open beauty ($\bar{b}q$ or $b\bar{q}$; $q \in u, d, s$) mesons, their mass spectra, as well as their decay properties in this paper. The study of B and B_s mesons also carries special interest as these hadrons with open flavors ($\bar{b}, u/d$ and \bar{b}, s) undergo flavor-changing decays with less interference from strong interaction decays. These particles thus provide a clean laboratory to study electromagnetic and weak interactions. Moreover, the understanding of the weak transition form factors of heavy mesons is important for proper extraction of the quark mixing parameters through the analysis of nonleptonic decays and CP -violating effects. QCD sum rules [16–19] is one of the nonperturbative approaches to evaluate hadron properties by using the correlator of the

*mnshah09@gmail.com

†azadpatel2003@gmail.com

‡p.c.vinodkumar@gmail.com

quark currents over the physical vacuum and it is implemented with the operator product expansion. Lattice QCD (LQCD) [20–26], another nonperturbative approach, employs a discrete set of spacetime points (lattice) to reduce the analytically intractable path integrals of the continuum theory to very complex numerical computations. While QCD sum rules are suitable for describing the low- q^2 region of the form factors, lattice QCD gives good predictions for high q^2 . As a result these methods do not provide a full picture of the form factors and, more significantly, for the relations between various decay channels. Potential models provide such relations and give the form factors in the full q^2 range.

Phenomenologically, the heavy mesons are composed of a heavy quark (b) or antiquark (\bar{b}) and a light quark (q) or antiquark (\bar{q}), in which quarks are treated as four-spinor Dirac particles. The heavy quark symmetry is taken into account consistently within a potential model. We believe that a quark potential model may still be effective if we treat the bound-state equation appropriately, which is capable of predicting not only mass differences but also absolute values of hadron masses. An equally mixed scalar plus vector potential in the Dirac equation can realize quark confinement to generate relativistic quark-antiquark bound states [27,28]. This analogy provides a simple way to make predictions for their excited states. In the limit $M_Q \rightarrow \infty$ heavy-light mesons can be characterized by the spin of the heavy quark, S_Q , the total angular momentum of the light quark, $\vec{j}_q = \vec{S}_q + \vec{L}$, and the total angular momentum, $\vec{J} = \vec{S}_Q + \vec{j}_q$. For P-wave excited states, there appear two degenerate doublets, one corresponding to $j_q = 1/2$ and the other to $j_q = 3/2$, with quantum numbers $J^P = 0^+, 1^+$ and $J^P = 1^+, 2^+$, respectively. Those states with $j_q = 1/2$ can only decay through an S-wave transition, whereas the $j_q = 3/2$ states undergo a D-wave transition. Therefore the decay widths are expected to be much broader for $j_q = 1/2$ than for $j_q = 3/2$ states. Further theoretical efforts are still required in order to satisfactorily explain the data concerning these open-beauty states.

Any attempt towards the identification of the newly observed states thus becomes very important for a better understanding of the quark-antiquark dynamics within the $Q\bar{q}$ bound state. So, a successful theoretical model can provide important information about the quark-antiquark interactions and the behavior of QCD within the doubly open flavor hadronic system. Though there exist many theoretical models [3–5,29] to study the hadron properties based on its quark structure, the predictions for low-lying states are off by 50–100 MeV. Moreover, the issues related to the hyperfine and fine-structure splitting of the mesonic states (i.e., their intricate dependence on the constituent quark masses and the running strong coupling constant) are still unresolved. Though nonrelativistic models are very

well established and significantly successful for the description of heavy quarkonia, disparities exist in the description of mesons containing light flavor quarks or antiquarks. The use of the nonrelativistic Schrödinger treatment to study their bound states may not be quite appropriate. Therefore, these open flavor mesons must be discussed in the framework of the relativistic formalism [28,30–34]. Thus, in the present work to study atom-like mesons $b\bar{q}$ or $q\bar{b}$, we employ the Dirac equation with an equally mixed 4-vector plus scalar power-law potential.

Apart from the successful predictions of the mass spectra, the validity of any phenomenological model depends also on the successful predictions of their decay properties. For better predictions of the decay widths, many models have incorporated additional contributions, such as radiative and higher-order QCD corrections [35–40]. In this paper we make an attempt to study properties like the mass spectrum, decay constants, and other flavor-changing decay properties of the B and B_s mesons based on a relativistic Dirac formalism. We investigate the heavy-light mass spectra of B and B_s mesons in this framework with a Martin-like confinement potential [28,34].

Along with the mass spectra, the pseudoscalar decay constants of the heavy-light mesons have also been estimated in the context of many QCD-motivated approximations. The predictions of all such attempts cover a wide range of values [41,42]. It is important to have a reliable estimate of the decay constant as it is an important parameter in many weak processes, such as quark mixing, CP violation, etc. The leptonic decay of a charged meson is another important annihilation channel through the exchange of a virtual W boson. Though this annihilation process is rare, they have clear experimental signatures due to the presence of highly energetic leptons in the final state. There also exist experimental observations of the leptonic decays of B and B_s mesons. The leptonic decays of mesons entail an appropriate representation of the initial state of the decaying vector mesons in terms of the constituent quark and antiquark with their respective momenta and spin. The bound constituent quark and antiquark inside the meson are in definite energy states having no definite momenta. However, one can find out the momentum distribution amplitude for the constituent quark and antiquark inside the meson immediately before their annihilation to a lepton pair. Thus, it is appropriate to compute the leptonic branching ratio and compare the result with the experimental values as well as with the predictions based on other models. Decays that are highly suppressed in the standard model are excellent places to search for effects of new physics. The rare decays $B_s^0 \rightarrow \mu^+\mu^-$ and $B^0 \rightarrow \mu^+\mu^-$ were discovered by the CMS and LHCb collaborations very recently [2,43–45]. Particle-antiparticle mixing is responsible for the small mass differences between the mass eigenstates of neutral mesons. Particle-antiparticle mixing has been the major important process in testing the

standard model, and this mixing is responsible for the small mass differences between the mass eigenstates of neutral mesons. The $B_d - \bar{B}_d$ mixing gave the first indication of a large top-quark mass and a perfect testing ground for heavy-flavor physics [46]. The present study on the various properties of B and B_s mesons are presented in different sections. In Sec. II, a review of the theoretical framework based on the Dirac formalism and the mass spectra of the B and B_s mesonic states are presented. In Sec. III, the electromagnetic transition rates of these mesonic states are computed and tabulated. The pseudoscalar decay constants and the calculational details are presented in Sec. IV. The details of computing the leptonic decays, rare decay of B_s^0 and B^0 mesons into dileptons, and their hadronic decays are given in Secs. V and VI, respectively. The mixing parameters of the $B_q^0 - \bar{B}_q^0$ and $B_s^0 - \bar{B}_s^0$ are discussed and presented in Sec. VII. Finally, in Sec. VIII general conclusions and predictions of the present study are summarized and discussed.

II. THEORETICAL FRAMEWORK BASED ON THE DIRAC FORMALISM

The nonperturbative multigluon mechanism is unfeasible to estimate the quark confining interaction theoretically from the first principles of QCD. On the other hand, there exists ample experimental support for the quark structure of hadrons. This is the origin of phenomenological models which are proposed to understand the properties of hadrons and quark dynamics at the hadronic scale. To first approximation, the confining part of the interaction is believed to provide the zeroth-order quark dynamics inside the meson through the quark Lagrangian density

$$\mathcal{L}_q^0(x) = \bar{\psi}_q(x) \left[\frac{i}{2} \gamma^\mu \vec{\partial}_\mu - V(r) - m_q \right] \psi_q(x). \quad (1)$$

For the present study, we assume that the constituent quark-antiquark inside a meson is independently confined by an average potential of the form [28,47]

$$V(r) = \frac{1}{2} (1 + \gamma_0) (\lambda r^\nu + V_0), \quad (2)$$

where λ is the potential strength and ν is the exponent of the power potential. For the Martin-like potential, we take the index $\nu = 0.1$. In the stationary case, the spatial part of the quark wave functions $\psi(\vec{r})$ satisfies the Dirac equation given by

$$[\gamma^0 E_q - \vec{\gamma} \cdot \vec{P} - m_q - V(r)] \psi_q(\vec{r}) = 0. \quad (3)$$

The solution of the Dirac equation can be written in a two-component (positive and negative energies in the zeroth order) form as

$$\psi_{nlj}(r) = \begin{pmatrix} \psi_{nlj}^{(+)} \\ \psi_{nlj}^{(-)} \end{pmatrix}, \quad (4)$$

where

$$\psi_{nlj}^{(+)}(\vec{r}) = N_{nlj} \begin{pmatrix} ig(r)/r \\ (\sigma \cdot \hat{r})f(r)/r \end{pmatrix} \mathcal{Y}_{ljm}(\hat{r}), \quad (5)$$

$$\psi_{nlj}^{(-)}(\vec{r}) = N_{nlj} \begin{pmatrix} i(\sigma \cdot \hat{r})f(r)/r \\ g(r)/r \end{pmatrix} (-1)^{j+m_j-l} \mathcal{Y}_{ljm}(\hat{r}), \quad (6)$$

and N_{nlj} is the overall normalization constant. The normalized spin angular part is given by

$$\mathcal{Y}_{ljm}(\hat{r}) = \sum_{m_l, m_s} \left\langle l, m_l, \frac{1}{2}, m_s | j, m_j \right\rangle Y_l^{m_l} \chi_{\frac{1}{2}}^{m_s}. \quad (7)$$

Here the spinor $\chi_{\frac{1}{2}m_s}$ represents the spin operators,

$$\chi_{\frac{1}{2}\frac{1}{2}} = \begin{pmatrix} 1 \\ 0 \end{pmatrix}, \quad \chi_{\frac{1}{2}-\frac{1}{2}} = \begin{pmatrix} 0 \\ 1 \end{pmatrix}. \quad (8)$$

The reduced radial part $g(r)$ of the upper component and $f(r)$ of the lower component of the Dirac spinor $\psi_{nlj}(r)$ satisfy the equations given by

$$\frac{d^2 g(r)}{dr^2} + \left[(E_D + m_q)[E_D - m_q - V(r)] - \frac{\kappa(\kappa + 1)}{r^2} \right] g(r) = 0 \quad (9)$$

and

$$\frac{d^2 f(r)}{dr^2} + \left[(E_D + m_q)[E_D - m_q - V(r)] - \frac{\kappa(\kappa - 1)}{r^2} \right] f(r) = 0. \quad (10)$$

On transforming into a convenient dimensionless form, we get [48]

$$\frac{d^2 g(\rho)}{d\rho^2} + \left[\epsilon - \rho^{0.1} - \frac{\kappa(\kappa + 1)}{\rho^2} \right] g(\rho) = 0 \quad (11)$$

and

$$\frac{d^2 f(\rho)}{d\rho^2} + \left[\epsilon - \rho^{0.1} - \frac{\kappa(\kappa - 1)}{\rho^2} \right] f(\rho) = 0, \quad (12)$$

where $\rho = (r/r_0)$ is a dimensionless variable with the arbitrary scale factor chosen conveniently as

$$r_0 = \left[(m_q + E_D) \frac{\lambda}{2} \right]^{-\frac{10}{21}}, \quad (13)$$

and ϵ is a corresponding dimensionless energy eigenvalue defined as

$$\epsilon = (E_D - m_q - V_0)(m_q + E_D)^{\frac{1}{2}} \left(\frac{2}{\lambda}\right)^{\frac{30}{\pi}}. \quad (14)$$

Here, it is suitable to define a quantum number κ by

$$\kappa = \begin{cases} -(\ell + 1) = -(j + \frac{1}{2}) & \text{for } j = \ell + \frac{1}{2}, \\ \ell = +(j + \frac{1}{2}) & \text{for } j = \ell - \frac{1}{2}. \end{cases} \quad (15)$$

Equations (11) and (12) now can be solved numerically [35] for each choice of κ .

The solutions $g(\rho)$ and $f(\rho)$ are normalized to get

$$\int_0^\infty (f_q^2(\rho) + g_q^2(\rho)) d\rho = 1. \quad (16)$$

The wave functions for B and B_s mesons now can be constructed using Eqs. (5) and (6) and the corresponding mass of the quark-antiquark system can be written as

$$M_{Q\bar{q}} = E_D^Q + E_{\bar{q}}^{\bar{q}}, \quad (17)$$

where $E_D^{Q/\bar{q}}$ are obtained using Eqs. (14) and (15) which also include the centrifugal repulsion of the center of mass. For the spin triplet (vector) and spin singlet (pseudoscalar) states, the choices of (j_1, j_2) are $((l_1 + \frac{1}{2}), (l_2 + \frac{1}{2}))$ and $((l_{1,2} + \frac{1}{2}), (l_{2,1} - \frac{1}{2}))$, respectively. The previous work with the independent quark model within the Dirac formalism in Refs. [28,47] has been extended here by incorporating the spin-orbit and tensor interactions of the confined one-gluon exchange potential (COGEP) [49,50], in addition to the $j-j$ coupling of the quark-antiquark. Finally, the mass of the specific $^{2S+1}L_J$ states of the $Q\bar{q}$ system is expressed as

$$M_{2S+1L_J} = M_{Q\bar{q}}(n_1 l_1 j_1, n_2 l_2 j_2) + \langle V_{Q\bar{q}}^{j_1 j_2} \rangle + \langle V_{Q\bar{q}}^{LS} \rangle + \langle V_{Q\bar{q}}^T \rangle. \quad (18)$$

The spin-spin part is defined here as

$$\langle V_{Q\bar{q}}^{j_1 j_2}(r) \rangle = \frac{\sigma \langle j_1 j_2 JM | \hat{j}_1 \cdot \hat{j}_2 | j_1 j_2 JM \rangle}{(E_Q + m_Q)(E_{\bar{q}} + m_{\bar{q}})}, \quad (19)$$

where σ is the $j-j$ coupling constant. The expectation value of $\langle j_1 j_2 JM | \hat{j}_1 \cdot \hat{j}_2 | j_1 j_2 JM \rangle$ contains the (j_1, j_2) coupling and the square of the Clebsch-Gordan coefficients. The tensor and spin-orbit parts of the COGEP [49,50] are given by

$$V_{Q\bar{q}}^T(r) = -\frac{\alpha_s}{4} \frac{N_Q^2 N_{\bar{q}}^2}{(E_Q + m_Q)(E_{\bar{q}} + m_{\bar{q}})} \otimes \lambda_Q \cdot \lambda_{\bar{q}} \left(\left(\frac{D_1''(r)}{3} - \frac{D_1'(r)}{3r} \right) S_{Q\bar{q}} \right), \quad (20)$$

where $S_{Q\bar{q}} = [3(\sigma_Q \cdot \hat{r})(\sigma_{\bar{q}} \cdot \hat{r}) - \sigma_Q \cdot \sigma_{\bar{q}}]$, $\hat{r} = \hat{r}_Q - \hat{r}_{\bar{q}}$ is the unit vector in the direction of \vec{r} , and

$$V_{Q\bar{q}}^{LS}(r) = \frac{\alpha_s}{4} \frac{N_Q^2 N_{\bar{q}}^2}{(E_Q + m_Q)(E_{\bar{q}} + m_{\bar{q}})} \frac{\lambda_Q \cdot \lambda_{\bar{q}}}{2r} \otimes [[\vec{r} \times (\hat{p}_Q - \hat{p}_{\bar{q}}) \cdot (\sigma_Q + \sigma_{\bar{q}})] (D_0'(r) + 2D_1'(r)) + [\vec{r} \times (\hat{p}_Q + \hat{p}_{\bar{q}}) \cdot (\sigma_Q - \sigma_{\bar{q}})] (D_0'(r) - D_1'(r))], \quad (21)$$

where α_s is the strong coupling constant and it is computed as

$$\alpha_s = \frac{4\pi}{(11 - \frac{2}{3}n_f) \log(\frac{M_Z^2}{\Lambda_{\text{QCD}}^2})}. \quad (22)$$

Here $n_f = 4$ and $\Lambda_{\text{QCD}} = 0.156$ GeV provide us with the experimentally known value for α_s at the Z meson mass range of 0.118. In Eq. (21) the spin-orbit term has been split into symmetric $(\sigma_Q + \sigma_{\bar{q}})$ and antisymmetric $(\sigma_Q - \sigma_{\bar{q}})$ parts.

We have adopted the same parametric form of the confined gluon propagators as in Refs. [49,50],

$$D_0(r) = \left(\frac{\alpha_1}{r} + \alpha_2 \right) \exp(-r^2 c_0^2 / 2) \quad (23)$$

and

$$D_1(r) = \frac{\gamma}{r} \exp(-r^2 c_1^2 / 2), \quad (24)$$

with $\alpha_1 = 0.036$, $\alpha_2 = 0.056$, $c_0 = 0.1017$ GeV, $c_1 = 0.1522$ GeV, and $\gamma = 0.0139$ as in the earlier study [28]. Other optimized model parameters employed in the present study are listed in Table I. The computed S-wave masses and other P-wave and D-wave masses of B meson states are listed in Tables II and III, respectively, and the corresponding B_s meson states are listed in Tables IV and V, respectively. A statistical analysis of the sensitivity of the model parameters [i.e., the potential strength (λ) and $j-j$ coupling strength σ in the present case] shows about 3% and 30% variations in the binding energy with 10% changes in the parameters λ and σ , respectively. Figures 1 and 2 show the energy level diagrams of B and B_s meson spectra along with the reported experimental results.

TABLE I. The fitted model parameters for the B and B_s systems.

System parameters	B	B_s
Quark mass (in GeV)	$m_{u,d} = 0.003$ and $m_b = 4.67$	$m_s = 0.1$ and $m_b = 4.67$
Potential strength (λ)	$2.3756 + A\text{GeV}^{\nu+1}$	$2.3756 + A\text{GeV}^{\nu+1}$
V_0	-2.6461 GeV	-2.6461 GeV
Centrifugal parameter (A)	$(n * 0.103)$ $\text{GeV}^{\nu+1}$ for $l = 0$ $((n + l) * 0.086)$ $\text{GeV}^{\nu+1}$ for $l \neq 0$	$(n * 0.1186)$ $\text{GeV}^{\nu+1}$ for $l = 0$ $((n + l) * 0.091)$ $\text{GeV}^{\nu+1}$ for $l \neq 0$
σ ($j - j$ coupling strength)	-0.732 GeV^3 for $l = 0$ -0.7961 GeV^3 for $l \neq 0$	-0.995 GeV^3 for $l = 0$ -1.254 GeV^3 for $l \neq 0$

TABLE II. S-wave B ($b\bar{q}$, $q \in u, d$) spectrum (in MeV).

nL	J^P	State	$M_{Q\bar{q}}$	$\langle V_{Q\bar{q}}^{j_1 j_2} \rangle$	Present	Experiment								
						Meson	Mass [1]	[51]	[52]	[11]	[5]	[53]	[25]	[26]
1S	1^-	1^3S_1	5360.21	-34.98	5325.23	B^*	5325.2 ± 0.4	5330	5326	5330	5324	5325	5325	5321
	0^-	1^1S_0	5191.38	87.97	5279.36	B	5279.58 ± 0.17	5280	5280	5266	5279	5277	5279	5291
2S	1^-	2^3S_1	5847.79	-23.89	5823.90		...	5870	5906	5946	5920	5848
	0^-	2^1S_0	5748.46	55.76	5804.22		...	5830	5890	5930	5886	5822
3S	1^-	3^3S_1	6272.08	-18.49	6253.58		...	6240	6387	6396	6347	6136
	0^-	3^1S_0	6199.61	42.46	6242.07		...	6210	6379	6387	6320	6117
4S	1^-	4^3S_1	6664.61	-15.18	6649.43		6786	6779	...	6351
	0^-	4^1S_0	6606.55	34.61	6641.17		...	6520	6781	6773	...	6335

[51] Heavy quark effective theory

[52] Quasipotential approach

[11] Relativistic quark-antiquark potential (Coulomb plus power) model

[5] The chiral quark model

[53] The nonrelativistic approach (Blankenbecler-Sugar equation)

[25] Lattice QCD (HPQCD Collaboration)

[26] Lattice QCD (UKQCD Collaboration)

TABLE III. S-wave B_s ($b\bar{s}$) spectrum (in MeV).

nL	J^P	State	$M_{Q\bar{q}}$	$\langle V_{Q\bar{q}}^{j_1 j_2} \rangle$	Present	Experiment								
						Meson	Mass [1]	[51]	[52]	[11]	[5]	[53]	[25]	[26]
1S	1^-	1^3S_1	5451.61	-36.19	5415.42	B_s^*	$5415.4^{+2.4}_{-2.1}$	5430	5414	5417	5421	5417	5430	5409
	0^-	1^1S_0	5277.53	88.92	5366.45	B_s	5366.77 ± 0.24	5370	5372	5355	5373	5366	5380	5382
2S	1^-	2^3S_1	5982.04	-25.89	5956.15		...	5970	5992	6016	6019	5966
	0^-	2^1S_0	5879.22	60.02	5939.24		...	5930	5976	5998	5985	5939
3S	1^-	3^3S_1	6447.69	-20.48	6427.20		...	6340	6475	6449	6449	6274
	0^-	3^1S_0	6372.25	46.88	6419.14		...	6310	6467	6441	6421	6254
4S	1^-	4^3S_1	6881.33	-17.03	6864.30		6879	6818	...	6504
	0^-	4^1S_0	6820.60	38.75	6859.35		...	6620	6874	6812	...	6487

[51] Heavy quark effective theory

[52] Quasipotential approach

[11] Relativistic quark-antiquark potential (Coulomb plus power) model

[5] The chiral quark model

[53] The nonrelativistic approach (Blankenbecler-Sugar equation)

[25] Lattice QCD (HPQCD Collaboration)

[26] Lattice QCD (UKQCD Collaboration)

TABLE IV. P-wave and D-wave B ($b\bar{q}$, $q \in u, d$) spectrum (in MeV).

nL	J^P	State	$M_{Q\bar{q}}$	$\langle V_{Q\bar{q}}^{ijj_2} \rangle$	$\langle V^T \rangle$	$\langle V^{LS} \rangle$	Present	Experiment						
								Meson	Mass [1]	[51]	[52]	[11]	[5]	[53]
1P	2^+	1^3P_2	5695.18	44.15	-1.18	15.36	5753.51	$B_2(5747)$	5743 ± 5	5710	5741	5779	5714	5704
	1^+	1^3P_1	5695.18	36.79	5.90	-15.36	5722.51	$B_1(5721)$	5723.5 ± 2.0	5690	5723	5764	5700	5686
	0^+	1^3P_0	5695.18	44.15	-11.80	-30.71	5696.81	$B_0(5732)$	5698 ± 8	5650	5749	5746	5706	5678
									5710 ± 20 [54]					
	1^+	1^1P_1	5597.49	140.07	0	0	5737.56		...	5690	5774	5785	5742	5699
2P	2^+	2^3P_2	6094.10	33.98	-2.09	27.22	6153.21		...	6120	6260	6255	6188	6040
	1^+	2^3P_1	6094.10	28.31	10.45	-27.22	6105.63		...	6100	6209	6243	6175	6022
	0^+	2^3P_0	6094.10	33.98	-20.89	-54.45	6052.73		...	6060	6221	6225	6163	6010
	1^+	2^1P_1	6026.94	103.90	0	0	6130.84		...	6100	6281	6256	6194	6028
3P	2^+	3^3P_2	6453.96	27.92	-2.96	38.63	6517.54	
	1^+	3^3P_1	6453.96	23.26	14.82	-38.63	6453.41	
	0^+	3^3P_0	6453.96	27.92	-29.63	-77.26	6374.98	
	1^+	3^1P_1	6402.15	84.13	0	0	6486.28	
1D	3^-	1^3D_3	6030.16	10.59	-0.006	0.104	6040.85		...	5970	6091	6060	5993	5871
	2^-	1^3D_2	6030.16	35.31	0.021	-0.048	6065.44		...	5960	6103	6056	5985	5920
	1^-	1^3D_1	6030.16	74.14	-0.021	-0.145	6104.14		...	5970	6119	6114	6025	6005
	2^-	1^1D_2	5953.77	122.46	0	0	6076.23		...	5980	6121	6125	6037	5955
2D	3^-	2^3D_3	6399.88	8.61	-0.003	0.052	6408.54		...	6320	6542	6479	...	6140
	2^-	2^3D_2	6399.88	28.70	0.011	-0.026	6428.56		...	6310	6528	6476	...	6179
	1^-	2^3D_1	6399.88	60.27	-0.011	-0.078	6460.06		...	6240	6534	6522	...	6248
	2^-	2^1D_2	6342.04	97.72	0	0	6439.76		...	6320	6554	6532	...	6207
3D	3^-	3^3D_3	6743.61	7.29	-0.007	0.111	6751.01	
	2^-	3^3D_2	6743.61	24.31	0.024	-0.056	6767.89	
	1^-	3^3D_1	6743.61	51.05	-0.024	-0.167	6794.47	
	2^-	3^1D_2	6696.63	82.02	0	0	6778.65	

Lattice QCD (HPQCD Collaboration) [25] results for $1^3P_2(2^+)$ (5723 MeV) and $1^1P_1(1^+)$ (5706 MeV).

Lattice QCD (UKQCD Collaboration) [26] results for $1^3P_2(2^+)$ (5821.8 ± 67 MeV), $1^3P_1(1^+)$ (5725.3 ± 58.9 MeV), and $1^3P_0(0^+)$ (5669 ± 53.6 MeV).

III. ELECTROMAGNETIC TRANSITIONS OF THE OPEN BEAUTY MESON

Spectroscopic studies allow one to compute the decay widths of energetically allowed radiative transitions of the type $A \rightarrow B + \gamma$ among several vector and pseudoscalar states of B and B_s mesons. The investigation of radiative transitions becomes important and such a study could help us understand the electromagnetic processes in the non-perturbative regime of QCD. The study of heavy-flavor mesonic systems allows us to apply the usual multipole expansion in electrodynamics to compute the transition between the B/B_s meson states with the emission of a photon. The leading terms in this expansion correspond to the E1 and M1 transitions. The electric dipole term (E1) is responsible for the transition between the S and P states without changing the spin of the quark-antiquark pair, while the magnetic dipole term (M1) describes the transition between $S = 1$ and $S = 0$ states without changing the relative orbital angular momentum (L) of the quark-antiquark pair. Accordingly, electric transitions do not change the quark spin. These transitions have $\Delta L = \pm 1$ and $\Delta S = 0$. The magnetic dipole transitions (M1) flip the

quark spin, so their amplitudes are proportional to the quark magnetic moments and thus related inversely to the quark mass. Thus, M1 transitions are weaker than the E1 transitions and this causes difficulties in the experimental observations. Along with other exclusive processes, M1 transitions from the spin-triplet S-wave vector (V) state to the spin-singlet S-wave pseudoscalar (P) state have also been considered as a valuable testing ground to further constrain the phenomenological quark model of hadrons. The E1 radiative transition width between the initial state ($n^{2s+1}L_J$) and the final state ($n'^{2s'+1}L''_{J'}$) is given by [55]

$$\Gamma(i \rightarrow f + \gamma) = \frac{4\alpha \langle e_Q \rangle^2}{3} (2J' + 1) S_{if}^E k^3 |\mathcal{E}_{if}|^2. \quad (25)$$

The M1 transitions have $\Delta L = 0$ and the $n^{2s+1}L_J \rightarrow n'^{2s'+1}L_{J'} + \gamma$ transition rate for the B_q system is given by [56–58]

$$\Gamma(i \rightarrow f + \gamma) = \frac{\alpha \mu^2}{3} (2J' + 1) S_{if}^M k^3 |\mathcal{M}_{if}|^2, \quad (26)$$

TABLE V. P-wave and D-wave B_s ($b\bar{s}$) spectrum (in MeV).

nL	J^P	State	$M_{Q\bar{q}}$	$\langle V_{Q\bar{q}}^{ijj_2} \rangle$	$\langle VT \rangle$	$\langle V^{LS} \rangle$	Present	Experiment						
								Meson	Mass [1]	[51]	[52]	[11]	[5]	[53]
1P	2^+	1^3P_2	5781.14	54.98	-1.04	13.49	5848.58	$B_{s2}(5840)$	5839.96 ± 0.20	5820	5842	5859	5820	5815
	1^+	1^3P_1	5781.14	45.82	5.18	-13.49	5818.65	$B_{s1}(5830)$	5828.7 ± 0.4	5800	5831	5845	5805	5795
	0^+	1^3P_0	5781.14	54.98	-10.38	-26.99	5798.75			5750	5833	5820	5804	5781
	1^+	1^1P_1	5681.66	172.11	0	0	5853.77	$B_{s1}(5850)$	5853 ± 15	5790	5865	5857	5842	5805
2P	2^+	2^3P_2	6196.28	21.85	-1.91	24.94	6241.16		...	6220	6359	6317	6292	6170
	1^+	2^3P_1	6196.28	16.03	9.57	-24.94	6196.93		...	6200	6345	6306	6278	6153
	0^+	2^3P_0	6196.28	43.71	-19.14	-49.88	6170.96		...	6170	6318	6283	6264	6143
	1^+	2^1P_1	6128.12	149.49	0	0	6277.61		...	6210	6321	6312	6296	6160
3P	2^+	3^3P_2	6571.22	18.32	-2.71	35.40	6622.23	
	1^+	3^3P_1	6571.22	13.43	13.58	-35.40	6562.83	
	0^+	3^3P_0	6571.22	36.64	-27.16	-70.81	6509.89	
	1^+	3^1P_1	6518.69	123.80	0	0	6642.50	
1D	3^-	1^3D_3	6131.41	13.55	-0.006	0.104	6145.06		...	6080	6191	6188	6103	6016
	2^-	1^3D_2	6131.41	45.18	0.022	-0.052	6176.56		...	6070	6189	6110	6095	6043
	1^-	1^3D_1	6131.41	94.88	-0.022	-0.156	6226.11		...	6070	6209	6188	6127	6094
	2^-	1^1D_2	6053.82	155.59	0	0	6209.41		...	6080	6218	6199	6140	6067
2D	3^-	2^3D_3	6516.40	11.26	-0.004	0.059	6527.72		...	6420	6637	6524	...	6298
	2^-	2^3D_2	6516.40	37.54	0.013	-0.029	6553.92		...	6410	6625	6517	...	6320
	1^-	2^3D_1	6516.40	78.84	-0.013	-0.089	6595.13		...	6340	6629	6579	...	6362
	2^-	2^1D_2	6457.72	127.34	0	0	6585.06		...	6420	6651	6588	...	6339
3D	3^-	3^3D_3	6874.79	9.68	-0.007	0.114	6884.58	
	2^-	3^3D_2	6874.79	32.27	0.024	-0.057	6907.03	
	1^-	3^3D_1	6874.79	67.78	-0.024	-0.170	6942.37	
	2^-	3^1D_2	6827.14	108.64	0	0	6935.78	

Lattice QCD (HPQCD Collaboration) [25] results for $1^3P_2(2^+)$ (5840 MeV) and $1^1P_1(1^+)$ (5828 MeV).

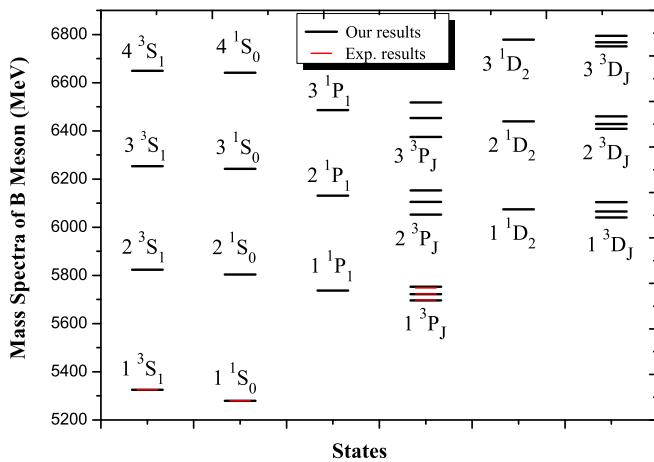
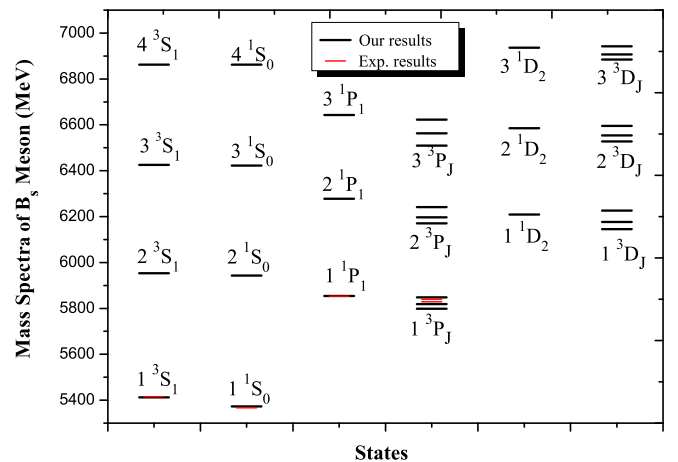
Lattice QCD (UKQCD Collaboration) [26] results for $1^3P_2(2^+)$ (5848.6 ± 61.6 MeV), $1^3P_1(1^+)$ (5786.9 ± 53.6 MeV), and $1^3P_0(0^+)$ (5722.6 ± 45.5 MeV).

where $\alpha = 1/137$, μ is the magnetic dipole moment and k is the photon energy, which are given by

$$\mu = \frac{m_{\bar{b}}e_q - m_q e_{\bar{b}}}{m_b m_{\bar{q}}}, \quad (27)$$

$$k = \frac{M_i^2 - M_f^2}{2M_i}, \quad (28)$$

and $\langle e_Q \rangle$ is the mean charge content of the open flavor (B_q) meson,

FIG. 1. B meson spectra.FIG. 2. B_s meson spectra.

$$\langle e_Q \rangle = \left| \frac{m_{\bar{b}} e_q - m_q e_{\bar{b}}}{m_b + m_{\bar{q}}} \right|. \quad (29)$$

Here, M_i and M_f are the initial- and final-state mass of the quarkonia, respectively, and $m_{q/\bar{b}}$ is the mass of the quark/antiquark. The statistical factors $S_{if}^E = S_{fi}^E$ and $S_{if}^M = S_{fi}^M$ are given by

$$S_{if}^E = \max(\ell, \ell') \left\{ \begin{matrix} J & 1 & J' \\ \ell' & s & \ell \end{matrix} \right\}^2, \quad (30)$$

$$S_{if}^M = 6(2s+1)(2s'+1) \left\{ \begin{matrix} J & 1 & J' \\ s' & \ell & s \end{matrix} \right\}^2 \left\{ \begin{matrix} 1 & \frac{1}{2} & \frac{1}{2} \\ \frac{1}{2} & s' & s \end{matrix} \right\}^2, \quad (31)$$

and the overlap integrals \mathcal{E}_{if} and \mathcal{M}_{if} are given by

$$\mathcal{E}_{if} = \mathcal{M}_{if} = \int_0^\infty dr u_{n\ell}(r) u_{n'\ell'}(r) \left[j_0 \left(\frac{kr}{2} \right) \right] \quad (32)$$

with their respective quantum numbers.

The computed E1 and M1 transition rates of B and B_s mesons are tabulated in Tables VIII and IX, respectively. The predicted radiative transition results are compared with other model predictions.

IV. DECAY CONSTANT OF B AND B_s MESONS

The decay constant of a meson is an important parameter in the study of leptonic or nonleptonic weak decay processes. The decay constant (f_p) of a pseudoscalar state is obtained by parametrizing the matrix elements of the weak current between the corresponding meson and the vacuum as [59]

$$\langle 0 | \bar{q} \gamma^\mu \gamma_5 c | P_\mu \rangle = i f_p P^\mu. \quad (33)$$

It is possible to express the quark-antiquark eigenmodes in the ground state of the meson in terms of the corresponding momentum distribution amplitudes. Accordingly, the eigenmodes $\psi_A^{(+)}$ in the state of definite momentum p and spin projection s'_p can be expressed as

$$\psi_A^{(+)} = \sum_{s'_p} \int d^3 p G_q(p, s'_p) \sqrt{\frac{m}{E_p}} U_q(p, s'_p) \exp(i\vec{p} \cdot \vec{r}), \quad (34)$$

where $U_q(p, s'_p)$ are the usual free Dirac spinors.

In the relativistic quark model, the decay constant can be expressed through the meson wave function $G_q(p)$ in the momentum space [60,61]

$$f_p = \left(\frac{3|I_p|^2}{2\pi^2 M_p J_p} \right)^{\frac{1}{2}}. \quad (35)$$

Here M_p is the mass of the pseudoscalar meson, and I_p and J_p are defined as

$$I_p = \int_0^\infty dp p^2 A(p) [G_{q1}(p) G_{q2}^*(-p)]^{\frac{1}{2}}, \quad (36)$$

$$J_p = \int_0^\infty dp p^2 [G_{q1}(p) G_{q2}^*(-p)], \quad (37)$$

respectively, where

$$A(p) = \frac{(E_{p1} + m_{q1})(E_{p2} + m_{q2}) - p^2}{[E_{p1} E_{p2} (E_{p1} + m_{q1})(E_{p2} + m_{q2})]^{\frac{1}{2}}} \quad (38)$$

and $E_{p_i} = \sqrt{k_i^2 + m_{q_i}^2}$.

The computed decay constants of the B and B_s mesons from 1S to 4S states are tabulated in Table X. The present result for the 1S state is compared with other theoretical model predictions. There are no predictions or measurements for a comparison of the decay constants of the 2S to 4S states.

V. DILEPTONIC DECAYS OF THE OPEN BEAUTY (B, B_s) MESON

Charged mesons produced from a quark and antiquark can decay to a charged lepton pair when these objects annihilate via a virtual W^\pm boson, as shown in Fig. 3. Though the leptonic decays of open flavor mesons belong to rare decay [62,63], they have clear experimental signatures due to the presence of a highly energetic lepton in the final state, and such decays are very clean due to the absence of hadrons in the final state [64]. The leptonic width of the B meson is computed using the relation [1]

$$\Gamma(B^+ \rightarrow l^+ \nu_l) = \frac{G_F^2}{8\pi} f_B^2 |V_{ub}|^2 m_l^2 \left(1 - \frac{m_l^2}{M_B^2} \right)^2 M_B, \quad (39)$$

in complete analogy to $\pi^+ \rightarrow l^+ \nu$. These transitions are helicity suppressed, i.e., the amplitude is proportional to

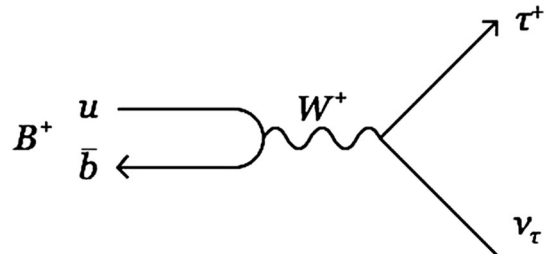


FIG. 3. Feynman diagram for leptonic decay ($M \rightarrow l \bar{\nu}_l$).

m_l , the mass of the lepton l . The leptonic widths of the B (1^1S_0) meson are obtained from Eq. (39) where the predicted values of the pseudoscalar decay constant f_B along with the masses of M_B and the Particle Data Group (PDG) value for $V_{ub} = 4.64 \times 10^{-3}$ are used. The leptonic widths for a separate lepton channel are computed for the choices of $m_{l=\tau,\mu,e}$. The branching ratios (BR) of these leptonic widths are then obtained as

$$\text{BR} = \Gamma(B^+ \rightarrow l^+ \nu_l) \times \tau, \quad (40)$$

where τ is the experimental lifetime of the respective B meson state. The computed leptonic widths are tabulated in Table XII along with other model predictions and available experimental values. Our results are found to be in accordance with the reported experimental values.

In the case of neutral B_s^0 and B^0 mesons, the single charge lepton decay is forbidden due to conservation of charge. The decay of these neutral mesons to two muons is also forbidden at the elementary level because the Z_0 cannot couple directly to quarks of different flavors and there are no direct flavor-changing neutral currents. But such decay occurs through higher-order transitions, such as those shown in Fig. 4. These are highly suppressed because each additional interaction vertex reduces their decay probability significantly. They are also helicity and Cabibbo-Kobayashi-Maskawa (CKM) suppressed. Consequently, the branching fraction for the $B_s^0 \rightarrow \mu^+ \mu^-$ and $B^0 \rightarrow \mu^+ \mu^-$ decay is expected to be very small compared to the dominant b antiquark to c antiquark transitions. Thus these dileptonic decays are considered as rare decays.

The decay width for rare decays of B_s^0 and B^0 mesons is given by [65–67]

$$\Gamma_{(B_q^0 \rightarrow \ell^+ \ell^-)} = \frac{G_F^2}{\pi} \frac{\alpha^2 f_{B_q}^2 m_\ell^2}{(4\pi \sin^2 \Theta_W)^2} m_{B_q} \times \sqrt{1 - 4 \frac{m_\ell^2}{m_{B_q}^2} |V_{ib}^* V_{iq}|^2} |C_{10}|^2. \quad (41)$$

The branching ratio for $B_q^0 \rightarrow \ell^+ \ell^-$ is

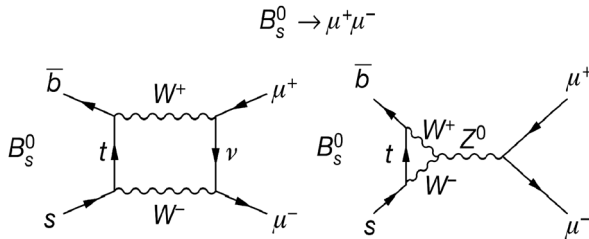


FIG. 4. Higher-order flavor-changing neutral current processes for the $B_s^0 \rightarrow \mu^+ \mu^-$ decay allowed in the standard model.

$$\text{BR} = \Gamma_{(B_q^0 \rightarrow \ell^+ \ell^-)} \times \tau_{B_q}. \quad (42)$$

G_F is the Fermi coupling constant, f_{B_q} is the corresponding decay constant, and C_{10} is the Wilson coefficient given by [67,68]

$$C_{10} = \eta_Y \frac{x_t}{8} \left[\frac{x_t + 2}{x_t - 1} + \frac{3x_t - 6}{(x_t - 1)^2} \ln x_t \right], \quad (43)$$

where $\eta_Y (= 1.026)$ is the next-to-leading-order correction [68] and $x_t = (m_t/m_w)^2$. In Eq. (41), $\Theta_W (\approx 28^\circ)$ is the weak mixing angle (Weinberg angle) [69]. The present results of these decays are tabulated in Table XIII along with available experimental values.

VI. HADRONIC DECAYS OF B AND B_s MESONS

The study of flavor-changing decays of heavy-flavor quarks are useful for determining the parameters of the standard model and for testing phenomenological models which include strong effects. The interpretation of the hadronic decays of B and B_s mesons within a hadronic state is complicated by the effects of the strong interaction and by its interplay with the weak interaction. The hadronic decays of heavy mesons can be understood in this model and we assume that Cabibbo-favored hadronic decays proceed via the basic process ($b \rightarrow q + u + \bar{d}$; $q \in s, d$), and the decay widths are given by [59]

$$\Gamma(B^0 \rightarrow D^- \pi^+ (\rho^+)) = C_f \frac{G_F^2 |V_{cb}|^2 |V_{ud}|^2 f_{\pi(\rho)}^2}{32\pi M_B^3} \times [\lambda(M_B^2, M_{D^-}^2, M_{\pi^+, \rho^+}^2)]^{\frac{3}{2}} |f_+(q^2)|, \quad (44)$$

$$\Gamma(B_s \rightarrow D_s^- \pi^+ (\rho^+)) = C_f \frac{G_F^2 |V_{cb}|^2 |V_{ud}|^2 f_{\pi(\rho)}^2}{32\pi M_B^3} \times [\lambda(M_B^2, M_{D_s^-}^2, M_{\pi^+, \rho^+}^2)]^{\frac{3}{2}} |f_+(q^2)| \quad (45)$$

and

$$\Gamma(B^0 \rightarrow D^{*-} \pi^+ (\rho^+)) = C_f \frac{G_F^2 |V_{cb}|^2 |V_{ud}|^2 f_{\pi(\rho)}^2}{32\pi M_B^3} \times [\lambda(M_B^2, M_{D^{*-}}^2, M_{\pi^+, \rho^+}^2)]^{\frac{3}{2}} |f_+(q^2)|, \quad (46)$$

$$\Gamma(B_s \rightarrow D_s^{*-} \pi^+ (\rho^+)) = C_f \frac{G_F^2 |V_{cb}|^2 |V_{ud}|^2 f_{\pi(\rho)}^2}{32\pi M_B^3} \times [\lambda(M_B^2, M_{D_s^{*-}}^2, M_{\pi^+, \rho^+}^2)]^{\frac{3}{2}} |f_+(q^2)| \quad (47)$$

for $b \rightarrow c$. Here, C_f is the color factor and ($|V_{ud}|, |V_{cb}|$) are the CKM matrices. f_π is the decay constant of the π meson and its value is taken as 0.130 GeV. Here, $f_+(q^2)$ is the form factor and the factors $\lambda(M_B^2, M_{D^-, D^{*-}}, M_{\pi^+, \rho^+}^2)$ and $\lambda(M_{B_s}^2, M_{D_s^-, D_s^{*-}}, M_{\pi^+, \rho^+}^2)$ can be computed as

$$\lambda(x, y, z) = x^2 + y^2 + z^2 - 2xy - 2yz - 2zx. \quad (48)$$

The renormalized color factor without the interference effect due to QCD is given by $(C_A^2 + C_B^2)$. The coefficients C_A and C_B are further expressed as [59]

$$C_A = \frac{1}{2}(C_+ + C_-), \quad (49)$$

$$C_B = \frac{1}{2}(C_+ - C_-), \quad (50)$$

where

$$C_+ = 1 - \frac{\alpha_s}{\pi} \log\left(\frac{M_W}{m_b}\right) \quad (51)$$

and

$$C_- = 1 + 2 \frac{\alpha_s}{\pi} \log\left(\frac{M_W}{m_b}\right), \quad (52)$$

where M_W is the mass of the W meson.

Consequently, the form factors $f_\pm(q^2)$ corresponding to the $b \rightarrow c$ are related to the Isgur-Wise function as, for instance, $B \rightarrow D\pi$ [59];

$$f_\pm(q^2) = \xi(\omega) \frac{M_B \pm M_D}{2\sqrt{M_B M_D}} \quad (53)$$

where the Isgur-Wise function, $\xi(\omega)$ can be evaluated according to the relation [70]

$$\xi(\omega) = \frac{2}{\omega - 1} \left\langle j_0 \left(2E_q \sqrt{\frac{\omega - 1}{\omega + 1}} r \right) \right\rangle, \quad (54)$$

where E_q is the binding energy of the decaying meson and ω is given by

$$\omega = \frac{M_B^2 + M_{(D^\pm, D^{*-})}^2 - q^2}{2M_B M_{(D^\pm, D^{*-})}}. \quad (55)$$

For a good approximation the form factor $f_-(q^2)$ does not contribute to the decay rate, so we have neglected it here. The heavy-flavor symmetry provides a model-independent normalization of the weak form factors $f_\pm(q^2)$ either at $q = 0$ or $q = q_{\max}$, and we have applied

$q = 0$ and $q = q_{\max}$ in Eq. (44) and $q = q_{\max}$ in Eq. (46) for hadronic decay. From the computed hadronic decay widths, the branching ratios are obtained as

$$\text{BR} = \Gamma \times \tau. \quad (56)$$

Here the lifetime (τ) of D ($\tau_{B^\pm} = 1.641 \text{ ps}^{-1}$ and $\tau_{B^0} = 1.519 \text{ ps}^{-1}$) is taken as the world average value reported by the Particle Data Group (PDG-2014) [1]. The computed decay widths and their branching ratios are listed in Table XIV along with the known experimental and other theoretical predictions for comparison.

VII. MIXING PARAMETERS OF $B^0 - \bar{B}^0$ AND $B_s^0 - \bar{B}_s^0$ OSCILLATION

Evidence of neutral open beauty meson ($B^0 - \bar{B}^0$, $B_s^0 - \bar{B}_s^0$) oscillations has been reported by three experimental groups [71–73]. Here, we study the mass oscillation of the neutral open beauty meson and the integrated oscillation rate using our spectroscopic parameters deduced from the present study. In the standard model, the transitions $B_q - \bar{B}_q$ and $\bar{B}_q - B_q$ occur through the weak interaction. The neutral B_q meson mixes with its antiparticle, leading to oscillations between the mass eigenstates [1]. In the following, we adopt the notation introduced in Ref. [1], and assume CPT conservation in our calculations. If CP symmetry is violated, the oscillation rates for a meson produced as B_q and \bar{B}_q can differ, further enriching the phenomenology. The study of CP violation in B^0 oscillation may lead to an improved understanding of possible dynamics beyond the standard model.

The time evolution of the neutral B_q -meson doublet is described by the Schrödinger equation with an effective 2×2 Hamiltonian given by [59,74]

$$i \frac{d}{dt} \begin{pmatrix} B_q(t) \\ \bar{B}_q(t) \end{pmatrix} = \left(M - \frac{i}{2} \Gamma \right) \begin{pmatrix} B_q(t) \\ \bar{B}_q(t) \end{pmatrix}, \quad (57)$$

where the \mathbf{M} and $\mathbf{\Gamma}$ matrices are Hermitian, and are defined as

$$\left(M - \frac{i}{2} \Gamma \right) = \left[\begin{pmatrix} M_{11}^q & M_{12}^{q*} \\ M_{12}^q & M_{11}^q \end{pmatrix} - \frac{i}{2} \begin{pmatrix} \Gamma_{11}^q & \Gamma_{12}^{q*} \\ \Gamma_{12}^q & \Gamma_{11}^q \end{pmatrix} \right]. \quad (58)$$

CPT invariance imposes

$$M_{11} = M_{22} \equiv M, \quad \Gamma_{11} = \Gamma_{22} \equiv \Gamma. \quad (59)$$

The off-diagonal elements of these matrices describe the dispersive and absorptive parts of $B_q - \bar{B}_q$ mixing [75]. The two eigenstates B_1 and B_2 of the effective Hamiltonian matrix $(M - \frac{i}{2} \Gamma)$ are given by

$$|B_1\rangle = \frac{1}{\sqrt{|p|^2 + |q|^2}}(p|B_q\rangle + q|\bar{B}_q\rangle), \quad (60)$$

$$|B_2\rangle = \frac{1}{\sqrt{|p|^2 + |q|^2}}(p|B_q\rangle - q|\bar{B}_q\rangle). \quad (61)$$

The corresponding eigenvalues are

$$\lambda_{B_1} \equiv m_1 - \frac{i}{2}\Gamma_1 = \left(M - \frac{i}{2}\Gamma\right) + \frac{q}{p} \left(M_{12} - \frac{i}{2}\Gamma_{12}\right), \quad (62)$$

$$\lambda_{B_2} \equiv m_2 - \frac{i}{2}\Gamma_2 = \left(M - \frac{i}{2}\Gamma\right) - \frac{q}{p} \left(M_{12} - \frac{i}{2}\Gamma_{12}\right), \quad (63)$$

where $m_1(m_2)$ and $\Gamma_1(\Gamma_2)$ are the mass and width of $B_1(B_2)$, respectively, and

$$\frac{q}{p} = \left(\frac{M_{12}^* - \frac{i}{2}\Gamma_{12}^*}{M_{12} - \frac{i}{2}\Gamma_{12}}\right)^{1/2}. \quad (64)$$

From Eqs. (62) and (63) one can get the differences in the mass and width, which are given as

$$\Delta m \equiv m_2 - m_1 = -2\text{Re}\left[\frac{q}{p} \left(M_{12} - \frac{i}{2}\Gamma_{12}\right)\right], \quad (65)$$

$$\Delta\Gamma \equiv \Gamma_2 - \Gamma_1 = -2\text{Im}\left[\frac{q}{p} \left(M_{12} - \frac{i}{2}\Gamma_{12}\right)\right]. \quad (66)$$

The calculation of the dispersive and absorptive parts of the box diagrams yields the following expressions for the off-diagonal element of the mass and decay matrices; for example, if s/\bar{s} is the intermediate quark state, then [75]

$$M_{12} = -\frac{G_F^2 m_W^2 \eta_{B_q} m_{B_q} B_{B_q} f_{B_q}^2}{12\pi^2} S_0(m_s^2/m_W^2) (V_{tq}^* V_{tb})^2, \quad (67)$$

$$\Gamma_{12} = \frac{G_F^2 m_b^2 \eta'_{B_q} m_{B_q} B_{B_q}}{f_{B_q}^2} 8\pi [(V_{tq}^* V_{tb})^2], \quad (68)$$

where G_F is the Fermi constant, m_W is the W boson mass, m_b is the mass of the b quark, and m_{B_q} , f_{B_q} , and B_{B_q} are the B_q mass, weak decay constant, and bag parameter, respectively. The known function $S_0(x_q)$ can be approximated very well by $0.784x_q^{0.76}$ [76] and V_{ij} are the elements of the CKM matrix [77]. The parameters η_{B_q} and η'_{B_q} correspond to the gluonic corrections. The only non-negligible contributions to M_{12} are from box

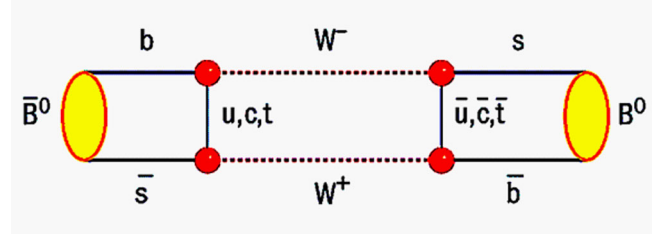


FIG. 5. $B^0 - \bar{B}^0$ mixing.

diagrams involving $u(\bar{u}), c(\bar{c})$ intermediate quarks in Figs. 5 and 6. The phases of M_{12} and Γ_{12} satisfy

$$\phi_M - \phi_\Gamma = \pi + \mathcal{O}\left(\frac{m_c^2}{m_b^2}\right), \quad (69)$$

implying that the mass eigenstates have mass and width differences of opposite signs. This means that, like in the $K^0 - \bar{K}^0$ system, the heavy state is expected to have a smaller decay width than that of the light state: $\Gamma_1 < \Gamma_2$. Hence, $\Delta\Gamma = \Gamma_2 - \Gamma_1$ is expected to be positive in the standard model. Further, the quantity

$$\left|\frac{\Gamma_{12}}{M_{12}}\right| \approx \frac{3\pi m_b^2}{2 m_W^2} \frac{1}{S_0(m_q^2/m_W^2)} \sim \mathcal{O}\left(\frac{m_q^2}{m_t^2}\right) \quad (70)$$

is small, and a power expansion of $|q/p|^2$ yields

$$\left|\frac{q}{p}\right|^2 = 1 + \left|\frac{\Gamma_{12}}{M_{12}}\right| \sin(\phi_M - \phi_\Gamma) + \mathcal{O}\left(\left|\frac{\Gamma_{12}}{M_{12}}\right|^2\right). \quad (71)$$

Therefore, considering both Eqs. (69) and (70), the CP -violating parameter given by

$$1 - \left|\frac{q}{p}\right|^2 \approx \text{Im}\left(\frac{\Gamma_{12}}{M_{12}}\right) \quad (72)$$

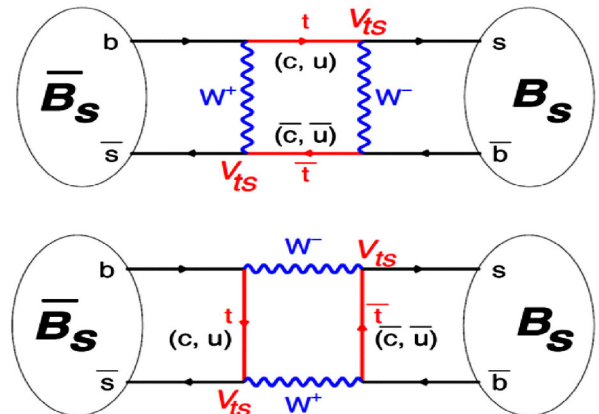


FIG. 6. $B_s - \bar{B}_s$ mixing.

is expected to be very small: $\sim \mathcal{O}(10^{-3})$ for the $B_q - \bar{B}_q$ system. In the approximation of negligible CP violation in mixing, the ratio $\Delta\Gamma/\Delta m$ is equal to the small quantity $|\Gamma_{12}/M_{12}|$ of Eq. (70); it is hence independent of the CKM matrix elements, i.e., the same for the $B_q - \bar{B}_q$ system.

Theoretically, the hadron lifetime (τ_{B_q}) is related to Γ_{11} ($\tau_{B_q} = 1/\Gamma_{11}$), while the observables Δm and $\Delta\Gamma$ are related to M_{12} and Γ_{12} as [1]

$$\Delta m = 2|M_{12}| \quad (73)$$

and

$$\Delta\Gamma = 2|\Gamma_{12}|. \quad (74)$$

The gluonic correction can be obtained by different means, like the Wilson coefficient and the evolution of the Wilson coefficient from the new physics scale [78]. We have used the values for the gluonic correction ($\eta_{B_d} = \eta'_{B_q} = 0.63$; $\eta_{B_s} = 0.51$, $\eta'_{B_s} = 0.55$) reported in Ref. [79]. The bag parameter $B_{B_d} = B_{B_s} = 1.34$ is taken from the lattice result of Ref. [80], while the pseudoscalar mass (M_{B_q}) and the pseudoscalar decay constant (f_{B_q}) of B_q mesons are the values obtained from our present study using a relativistic independent quark model with a Martin-like potential. The values of m_s (0.1 GeV), M_W (80.403 GeV), and the CKM matrix elements V_{td} (8.4×10^{-3}), V_{ts} (42.9×10^{-3}), and V_{tb} (0.89) are taken from the Particle Data Group [1]. The resulting mass oscillation parameter Δm is tabulated in Table XV along with the latest experimental results. The integrated oscillation rate (χ_q) is the probability to observe a \bar{B}_q meson in a jet initiated by a \bar{b} quark, as the mass difference Δm_{B_q} is a measure of the frequency of the change from a B_q into a \bar{B}_q or vice versa. This change is reflected in either the time-dependent oscillations or in the time-integrated rates corresponding to the dilepton events with the same sign. The time evolution of the neutral states from the pure $|B_{q\text{phys}}\rangle$ or $|\bar{B}_{q\text{phys}}\rangle$ state at $t = 0$ is given by

$$|B_{q\text{phys}}(t)\rangle = g_+(t)|B_q\rangle + \frac{q}{p}g_-(t)|\bar{B}_q\rangle, \quad (75)$$

$$|\bar{B}_{q\text{phys}}(t)\rangle = g_+(t)|\bar{B}_q\rangle + \frac{p}{q}g_-(t)|B_q\rangle, \quad (76)$$

which means that the flavor states remain unchanged (g_+) or oscillate into each other (g_-) with time-dependent probabilities proportional to

$$g_{\pm}(t) = e^{\mp\frac{\Gamma t}{2}} e^{-itm_{B_q}} \cos(t\Delta m/2), \quad (77)$$

$$g_{\pm}(t) = e^{\mp\frac{\Gamma t}{2}} e^{-itm_{B_q}} \sin(t\Delta m/2). \quad (78)$$

Starting at $t = 0$ with initially pure B_q , the probability of finding a B_q (\bar{B}_q) at time $t \neq 0$ is given by $|g_+(t)|^2$ ($|g_-(t)|^2$). Taking $|q/p| = 1$, one gets

$$|g_{\pm}(t)|^2 = \frac{1}{2} e^{-\frac{\Gamma t}{2}} [1 \pm \cos(t\Delta m)]. \quad (79)$$

The oscillation of B_q or \bar{B}_q as shown by Eq. (79) gives Δm directly. Integrating $|g_{\pm}(t)|^2$ from $t = 0$ to $t = \infty$, we get

$$\int_0^{\infty} |g_{\pm}(t)|^2 dt = \frac{1}{2} \left[\frac{1}{\Gamma} \pm \frac{\Gamma}{\Gamma^2 + (\Delta m)^2} \right], \quad (80)$$

where $\Gamma = \Gamma_{B_q} = (\Gamma_1 + \Gamma_2)/2$. The ratio

$$r_o = \frac{B_q \leftrightarrow \bar{B}_q}{B_q \leftrightarrow B_q} = \frac{\int_0^{\infty} |g_-(t)|^2 dt}{\int_0^{\infty} |g_+(t)|^2 dt} = \frac{x^2}{2 + x^2}, \quad \text{where}$$

$$x_q = x = \frac{\Delta m}{\Gamma} = \Delta m \tau_{B_q},$$

$$y_q = \frac{\Delta\Gamma}{2\Gamma} = \frac{\Delta\Gamma \tau_{B_q}}{2}, \quad (81)$$

$$\chi_q = \frac{x_q^2 + y_q^2}{2(x_q^2 + 1)}, \quad (82)$$

reflects the change of pure B_q into a \bar{B}_q , or vice versa. In the standard model, CP violation in beauty mixing is small and $|q/p| \approx 1$.

For the present estimation of the mixing parameters x_q , y_q , and χ_q , we employ our predicated Δm values and the experimental average lifetime from the PDG [1] of the B_q meson.

VIII. RESULTS AND DISCUSSION

We have studied the mass spectra and decay properties of open beauty mesons (B and B_s) in the framework of a relativistic independent quark model. Our computed B and B_s meson spectral states are in good agreement with the reported PDG values of known states. Though there are many experimentally known excited 1^- states of B and B_s mesons, most of them beyond $1S$ states are still not completely understood. And in the case of P-wave states only 1^3P_J of the B meson and 1^3P_2 , 1^3P_1 , 1^1P_1 of the B_s meson are known experimentally.

The predicted masses of the S-wave B meson states 2^3S_1 (5823.90 MeV) and 2^1S_0 (5804.22 MeV) are in accordance with other theoretical results. The predicted masses of the S-wave B_s meson states 2^3S_1 (5956.15 MeV) and 2^1S_0 (5939.24 MeV) are in accordance with other theoretical

results. We have also predicted the $3S$ and $4S$ states and compared them with the available theoretical results. The predicted P-wave B meson states 1^3P_2 (5753.80 MeV), 1^3P_1 (5721.16 MeV), and 1^3P_0 (5692.85 MeV) are in good agreement with experimental [1] results of 5743 ± 5 MeV, 5723.5 ± 2.0 MeV, and 5698 ± 8 MeV, respectively. The predicted P-wave B_s meson states 1^3P_2 (5849.52 MeV), 1^3P_1 (5818.02 MeV), and 1^1P_1 (5853.77 MeV) are in good agreement with experimental [1] results of 5839.96 ± 0.20 MeV, 5828.7 ± 0.4 MeV, and 5853 ± 15 MeV, respectively. The $2P, 1D, 2D$ states of B and B_s mesons were also calculated and compared with other theoretical results. We have predicted the $3P, 3D$ states of B and B_s mesons. One state, $B(5970)$, was recently observed by the CDF Collaboration [13–15], but their J^P values have yet to be confirmed. According to our analysis, $B(5970)$ is found to be a mixed state of 1^3D_1 (6105.12) and 2^3S_1 (5823.90) with a mixing angle of $(43.63)^\circ$.

In the relativistic Dirac formalism, the spin degeneracy is primarily broken; therefore, to have spin average masses of the different spectral states we employ the spin averaging procedure as

$$M_{CW} = \frac{\sum_J (2J+1) M_J}{\sum_J (2J+1)}. \quad (83)$$

The spin average or the c.m. masses M_{CW} of B and B_s mesons were calculated from the known values of the different meson states and are compared with other model predictions in Tables VI and VII. It also helps us

TABLE VI. Comparison of center of mass in the B meson in MeV.

M_{CW}	Present	[51]	[52]	[11]	[5]	[53]	Exp.
$\overline{1S}$	5313.76	5318	5315	5314	5313	5313	5313.8 ± 0.34
$\overline{2S}$	5818.98	5860	5902	5942	5912	5842	...
$\overline{3S}$	6250.70	6233	6385	6394	6340	6131	...
$\overline{4S}$	6647.36	...	6785	6778	...	6347	...
$\overline{1^3P_J}$	5736.15	5697	5736	5770	5708	5695	5732 ± 4
$\overline{1P}$	5735.88	5695	5745	5774	5717	5696	...

TABLE VII. Comparison of center of mass in the B_s meson in MeV.

M_{CW}	Present	[51]	[52]	[11]	[5]	[53]	Exp.
$\overline{1S}$	5403.17	5415	5404	5402	5409	5404	5313.8 ± 0.34
$\overline{2S}$	5951.92	5960	5988	6012	6011	5959	...
$\overline{3S}$	6425.19	6333	6473	6447	6442	6269	...
$\overline{4S}$	6863.06	...	6878	6817	...	6500	...
$\overline{1^3P_J}$	5833.07	5806	5837	5850	5813	5805	...
$\overline{1P}$	5838.24	5802	5844	5852	5820	5805	...

TABLE VIII. Magnetic (M1) transition of B and B_s mesons.

Transition	k (MeV)			Γ (keV)				
	Present	[83]	[81]	Present	[81]	[83]	[84]	[82]
$(1S)B^{*+} \rightarrow B^+\gamma$	45.67	45.800	45.24	0.65	0.65	1.63	0.19	0.42
$(1S)B^{*0} \rightarrow B^0\gamma$	45.67	45.800	45.24	0.16	0.21	0.92	0.07	0.14
$(1S)B_s^* \rightarrow B_s\gamma$	48.75	46.800	48.88	0.0007	0.13	0.71	0.05	0.09

to know the different spin-dependent contributions for the observed state.

The electromagnetic transitions (E1 and M1) can probe the internal charge and spin structure of hadrons, and therefore they will likely play an important role in determining the hadronic structures of B and B_s mesons. The present E1 and M1 transition widths of B and B_s meson states are listed in Tables VIII and IX, respectively. The present results of the M1 transition widths of B and B_s mesons are in accordance with the model prediction of Refs. [81] and [82], while there are no experimental results available. Our predictions and two other model predictions for M1 transitions are different because of their wave functions, and the corresponding overlap integrals may be different. We did not find more theoretical predictions for E1 and M1 transition widths for comparison. Thus we only look forward to see future experimental support for our predictions.

The calculated pseudoscalar decay constant (f_P) of B and B_s mesons are listed in Tables X and XI, along with other model predictions as well as experimental results. The value of $f_B(1S) = 188.56$ MeV obtained in our present study is in agreement with the experimental values [1] (206.7 ± 8.9). The value of $f_{B_s}(1S) = 240.21$ MeV obtained in our present study is in very good agreement with the lattice results and other theoretical models. The present values of the decay constant (f_P) of B and B_s mesons are also in accordance with other theoretical predictions for the $1S$ state. The predicted f_{B,B_s} for higher S-wave states are found to increase with energy.

TABLE IX. Electric (E1) transition of B and B_s mesons.

Transition	B Meson		B_s Meson	
	k (MeV)	Γ (keV)	k (MeV)	Γ (keV)
$1^3P_2(2^+) \rightarrow 1^3S_1(1^-) + \gamma$	411.75	0.463	415.370	0.5009
$1^3P_1(1^+) \rightarrow 1^3S_1(1^-) + \gamma$	384.69	0.378	389.267	0.4128
$1^3P_0(0^+) \rightarrow 1^3S_1(1^-) + \gamma$	363.39	0.319	372.878	0.3631
$1^1P_1(1^+) \rightarrow 1^1S_0(0^-) + \gamma$	411.59	0.585	464.660	0.7150
$2^3S_1(1^-) \rightarrow 1^3P_2(2^+) + \gamma$	70.587	0.0034	108.440	0.013
$2^3S_1(1^-) \rightarrow 1^3P_1(1^+) + \gamma$	99.239	0.0019	135.903	0.026
$2^3S_1(1^-) \rightarrow 1^3P_0(0^+) + \gamma$	121.603	0.0176	153.030	0.037
$2^1S_0(0^-) \rightarrow 1^1P_1(1^+) + \gamma$	64.468	0.0016	104.035	0.007

TABLE X. Pseudoscalar decay constant (f_P) of the B system (in MeV).

	f_P			
	1S	2S	3S	4S
Present	188.56	328.13	440.88	533.35
[QCDSR] [16]	186 ± 14			
[CPP $_\nu$] [10]	192			
[QCDSR] [17]	206 ± 7			
[RPM] [85]	198 ± 14			
[LFQM] [86]	204.0 ± 31			
[QCDSR] [18]	190 ± 17			
[QCDSR] [19]	207^{+17}_{-9}			
[LQCD] [20]	196.9 ± 9.1			
[LQCD] [21]	191 ± 9			
[LQCD] [22]	190 ± 13			
[LQCD] [23]	219 ± 17			
[LQCD] [24]	196.2 ± 15.7			

[QCDSR]- QCD sum rule
 [CPP $_\nu$]- Coloumb plus power potential model
 [RPM]- Relativistic potential model
 [LQCD]- Lattice QCD
 [LFQM]- Light-front quark model
 [RBSM]- Relativistic Bethe-Salpeter method

However, there are no experimental or theoretical values available for comparison. The ratio of the pseudoscalar decay constants f_{B_s}/f_B is also in good accord with other theoretical models listed in Table XI.

Another important property of B and B_s mesons studied in the present case is the leptonic decay widths. The present branching ratios for $B^+ \rightarrow \tau \bar{\nu}_\tau$ (1.354×10^{-4}), $B^+ \rightarrow \mu \bar{\nu}_\mu$ (6.085×10^{-7}), and $B^+ \rightarrow e \bar{\nu}_e$ (1.419×10^{-11}) are in excellent agreement with the experimental results ($1.65 \pm 0.34 \times 10^{-4}$, $< 1.0 \times 10^{-6}$, and $< 9.8 \times 10^{-7}$, respectively, over other theoretical predictions (see Table XII). A large experimental uncertainty in the muon and electron channel makes it difficult to develop any reasonable conclusion. We have predicted the decay widths and branching ratios of the rare leptonic decays $B_s^0 \rightarrow \ell^+ \ell^-$ and $B^0 \rightarrow \ell^+ \ell^-$ in Table XIII. The predicted branching ratios for $B_s^0 \rightarrow \mu^+ \mu^-$ (3.602×10^{-9}) and $B^0 \rightarrow \mu^+ \mu^-$ (1.018×10^{-10}) are in excellent agreement with the experimental results ($3.0^{+1.0}_{-0.9} \times 10^{-9}$ and $< 1.1 \times 10^{-9}$ [43], respectively. We have also predicted the branching ratios of other rare leptonic decays ($B_s^0 \rightarrow e^+ e^-$, $B_s^0 \rightarrow \tau^+ \tau^-$, $B^0 \rightarrow e^+ e^-$ and $B^0 \rightarrow \tau^+ \tau^-$). Here, it is difficult to make any reasonable conclusion because the large uncertainty in experimental results is present.

The Cabibbo-favored hadronic BRs $B^0 \rightarrow D^- \pi^+$, $B^0 \rightarrow D^{*-} \pi^+$, and $B_s \rightarrow D_s^- \rho^+$ obtained, respectively, as 3.724×10^{-3} , 3.475×10^{-3} , and 3.800×10^{-3} are in agreement with the PDG values of $(2.68 \pm 0.13) \times 10^{-3}$, $(2.76 \pm 0.13) \times 10^{-3}$, and $(7.4 \pm 1.7) \times 10^{-3}$, respectively. The BRs $B^0 \rightarrow D^- \rho^+$ (2.244×10^{-3}), $B^0 \rightarrow D^{*-} \rho^+$ (2.080×10^{-3}), $B_s \rightarrow D_s^- \pi^+$ (6.326×10^{-3}), $B_s \rightarrow D_s^{*-} \pi^+$ (5.833×10^{-3}), and $B_s \rightarrow D_s^- \rho^+$ (3.530×10^{-3}) are also in accord with the PDG values [1]

TABLE XI. Pseudoscalar decay constant (f_P) (in MeV) of the B_s system and ratio of the pseudoscalar decay constant.

	f_P				f_{B_s}/f_B
	1S	2S	3S	4S	1S
Present	240.21	393.61	521.26	614.28	1.27
[QCDSR] [16]	222 ± 12				1.19 ± 0.02 ± 0.04
[CPP $_\nu$] [10]	217				1.13
[QCDSR] [17]	234 ± 5				1.16 ± 0.05
[RPM] [85]	237 ± 17				1.197 ± 0.169
[LFQM] [86]	270.0 ± 47				1.32 ± 0.08
[QCDSR] [18]	233 ± 17				1.23 ± 0.12
[QCDSR] [19]	242.0^{+17}_{-12}				$1.169^{+0.178}_{-0.109}$
[LQCD] [20]	242.0 ± 10.0				1.229 ± 0.026
[LQCD] [21]	228 ± 10				1.188 ± 0.018
[LQCD] [22]	231 ± 15				1.226 ± 0.026
[LQCD] [23]	264 ± 19				1.193 ± 0.041
[LQCD] [24]	235.4 ± 12.2				1.193 ± 0.059

[QCDSR]- QCD sum rule
 [CPP $_\nu$]- Coloumb plus power potential model
 [RPM]- Relativistic potential model
 [LQCD]- Lattice QCD.
 [LFQM]- Light-front quark model

TABLE XII. The leptonic decay width and leptonic branching ratio of the B meson.

Process	$\Gamma(B^+ \rightarrow l^+ \nu_l)$ (keV)		BR			
	Present	[61]	Present	[11]	[61]	Experiment [1]
$B^+ \rightarrow \tau^+ \nu_\tau$	5.430×10^{-11}	3.77×10^{-14}	1.354×10^{-4}	1.07×10^{-4}	9.25×10^{-5}	$(1.65 \pm 0.34) \times 10^{-4}$
$B^+ \rightarrow \mu^+ \nu_\mu$	2.439×10^{-13}	1.69×10^{-16}	6.085×10^{-7}	4.82×10^{-7}	4.15×10^{-7}	$< 1.0 \times 10^{-6}$
$B^+ \rightarrow e^+ \nu_e$	5.689×10^{-18}	...	1.419×10^{-11}	1.13×10^{-11}	...	$< 9.8 \times 10^{-7}$

TABLE XIII. The rare leptonic decay width and branching ratio of the B^0 and B_s^0 mesons.

Process	$\Gamma(B_q^0 \rightarrow l^+ l^-)$ (keV)		BR		
	Present	Present	[65]	[87]	Experiment
$B_s^0 \rightarrow \mu^+ \mu^-$	1.583×10^{-15}	3.602×10^{-9}	$(3.65 \pm 0.23) \times 10^{-9}$	3.40×10^{-9}	$(3.1 \pm 0.7) \times 10^{-9}$ [1] $3.0_{-0.9}^{+1.0} \times 10^{-9}$ [43] [CMS] $3.2_{-1.2}^{+1.5} \times 10^{-9}$ [44] [LHCb] $2.9_{-1.0}^{+1.1} \times 10^{-9}$ [45] [LHCb]
$B_s^0 \rightarrow \tau^+ \tau^-$	3.361×10^{-13}	7.647×10^{-7}	$(7.73 \pm 0.49) \times 10^{-7}$	7.22×10^{-7}	
$B_s^0 \rightarrow e^+ e^-$	3.695×10^{-20}	8.408×10^{-14}	$(8.54 \pm 0.55) \times 10^{-14}$	7.97×10^{-14}	$< 2.8 \times 10^{-7}$
$B^0 \rightarrow \mu^+ \mu^-$	4.406×10^{-17}	1.018×10^{-10}	$(1.06 \pm 0.09) \times 10^{-10}$	1.20×10^{-10}	$< 6.3 \times 10^{-10}$ $< 1.1 \times 10^{-9}$ [43] [CMS] $< 9.4 \times 10^{-10}$ [44] [LHCb] $< 7.4 \times 10^{-10}$ [45] [LHCb]
$B^0 \rightarrow \tau^+ \tau^-$	9.232×10^{-15}	2.133×10^{-8}	$(2.22 \pm 0.19) \times 10^{-8}$	2.52×10^{-8}	$< 4.1 \times 10^{-3}$
$B^0 \rightarrow e^+ e^-$	1.028×10^{-21}	2.376×10^{-15}	$(2.48 \pm 0.21) \times 10^{-15}$	2.82×10^{-15}	$< 8.3 \times 10^{-8}$

TABLE XIV. The hadronic decay width and branching ratio of the B and B_s mesons.

Process	$\Gamma(D)$ (keV)		BR		Experiment [1]
	Present	Present (WCF)	Present (CF)		
$B^0 \rightarrow D^- \pi^+$	1.613×10^{-15}	3.724×10^{-3}	4.155×10^{-3}		$(2.68 \pm 0.13) \times 10^{-3}$
$B^0 \rightarrow D^{*-} \pi^+$	1.505×10^{-15}	3.475×10^{-3}	3.877×10^{-3}		$(2.76 \pm 0.13) \times 10^{-3}$
$B^0 \rightarrow D^- \rho^+$	0.971×10^{-15}	2.244×10^{-3}	2.504×10^{-3}		$(7.8 \pm 1.3) \times 10^{-3}$
$B^0 \rightarrow D^{*-} \rho^+$	0.901×10^{-15}	2.080×10^{-3}	2.321×10^{-3}		$(6.8 \pm 0.9) \times 10^{-3}$
$B_s \rightarrow D_s^- \pi^+$	2.780×10^{-15}	6.326×10^{-3}	7.058×10^{-3}		$(3.2 \pm 0.4) \times 10^{-3}$
$B_s \rightarrow D_s^{*-} \pi^+$	2.585×10^{-15}	5.833×10^{-3}	6.508×10^{-3}		$(2.1 \pm 0.6) \times 10^{-3}$
$B_s \rightarrow D_s^- \rho^+$	1.670×10^{-15}	3.800×10^{-3}	4.240×10^{-3}		$(7.4 \pm 1.7) \times 10^{-3}$
$B_s \rightarrow D_s^{*-} \rho^+$	1.542×10^{-15}	3.530×10^{-3}	3.938×10^{-3}		$(1.03 \pm 0.26) \times 10^{-2}$

(WCF): without color factor; (CF): with color factor.

$(7.8 \pm 1.3) \times 10^{-3}$, $(6.8 \pm 0.9) \times 10^{-3}$, $(3.2 \pm 0.4) \times 10^{-3}$, $(2.1 \pm 0.6) \times 10^{-3}$, and $(1.03 \pm 0.26) \times 10^{-2}$, respectively, but the percentage variations with experimental values are more than 55%. Here we have compared the results of the hadronic branching ratios with and without the color factor for comparison with experimental results. The hadronic BRs with and without the color factor are listed in Table XIV.

We obtained the CP violation parameter in mixing $|q/p|$ (0.9996) in this case, and $B^0 - \bar{B}^0$ and $B_s - \bar{B}_s$ decays show

no evidence for CP violation and provide the most stringent bounds on the mixing parameters. Our predicted mass differences Δm_{B_d} (0.506 ps^{-1}) and Δm_{B_s} (17.644 ps^{-1}) are in very good agreement with the experimental values [1] ($0.507 \pm 0.004 \text{ ps}^{-1}$ and $(17.69 \pm 0.08) \text{ ps}^{-1}$, respectively. The values of the mixing parameter x_q for $B^0 - \bar{B}^0$ (0.769) and $B_s - \bar{B}_s$ (26.41) are in very good agreement with the experimental values [1] 0.770 ± 0.008 and 26.49 ± 0.29 , respectively, and we have compared the mixing parameter

TABLE XV. Mixing parameters x_q , y_q , and χ_q of B and B_s mesons.

Meson		$\Delta M(\text{ps}^{-1})$	x_q	y_q	χ_q
B	Present	0.506	0.769	2.412×10^{-3}	0.1859
	Experiment [1]	0.507 ± 0.004	0.770 ± 0.008	...	0.1862 ± 0.0023
	[10]	0.520	0.7898	4.000×10^{-3}	0.1921
	[11]	0.498	0.759	2.600×10^{-3}	0.1827
	[22]	0.507 ± 0.005
	[73]	0.53 ± 0.02
B_s	Present	17.644	26.41	0.089	0.49929
	Experiment [1]	17.69 ± 0.08	26.49 ± 0.29	...	0.499292 ± 0.000016
	[10]	17.67	25.79	0.1308	0.4993
	[11]	20.286	29.862	0.1041	0.4994
	[22]	$17.77 \pm 0.10 \pm 0.07$
	[71]	$17.31^{+0.33}_{-0.18} \pm 0.07$
	[72]	$17.77 \pm 0.10 \pm 0.07$
	[73]	17.40

x_q with available theoretical results, as shown in Table XV. The large value of the mixing parameter obtained for the $B^0 - \bar{B}^0$ systems implies the maximal mixing with $\chi_d = 0.1859$ and the result is in very good agreement with the PDG value 0.1862 ± 0.0023 [1]. Similarly, the parameter $\chi_s = 0.49929$ for the $B_s - \bar{B}_s$ mixing is found to be in very good agreement with the PDG value of 0.499292 ± 0.000016 [1]. Thus, the present study of the mixing parameters of neutral open beauty mesons is a successful attempt to extract the effective quark-antiquark interaction in the case of heavy-light beauty mesons. Thus the present study is an attempt to indicate the importance of spectroscopic (strong interaction) parameters in the weak decay processes.

In conclusion, we have reported a comprehensive study of decay properties of the open beauty mesons. Many of the properties are expected to be used as guidelines to understand future experimental observations.

ACKNOWLEDGMENTS

The work is part of Major research project No. F. 40-457/2011(SR) funded by University Grant Commission, Gov. of India, India. One of the authors (B. P.) acknowledges the support through the Fast Track project funded by Department of Science and Technology, Ministry of Science and Technology (SR/FTP/PS-52/2011).

-
- [1] K. A. Olive *et al.* (Particle Data Group), *Chin. Phys. C* **38**, 090001 (2014); J. Beringer *et al.* (Particle Data Group), *Phys. Rev. D* **86**, 010001 (2012).
- [2] V. Khachatryan *et al.* (CMS and LHCb Collaborations), *Nature (London)* **522**, 68 (2015).
- [3] S. Godfrey and N. Isgur, *Phys. Rev. D* **32**, 189 (1985).
- [4] S. Godfrey and R. Kokoski, *Phys. Rev. D* **43**, 1679 (1991).
- [5] M. Di Pierro and E. Eichten, *Phys. Rev. D* **64**, 114004 (2001).
- [6] W. A. Bardeen, E. J. Eichten, and C. T. Hill, *Phys. Rev. D* **68**, 054024 (2003).
- [7] P. Colangelo, F. De Fazio, and R. Ferrandes, *Nucl. Phys. B, Proc. Suppl.* **163**, 177 (2007).
- [8] A. F. Falk and T. Mehen, *Phys. Rev. D* **53**, 231 (1996).
- [9] E. J. Eichten, C. T. Hill, and C. Quigg, *Phys. Rev. Lett.* **71**, 4116 (1993).
- [10] B. Patel and P. C. Vinodkumar, *J. Phys. G* **36**, 115003 (2009).
- [11] N. Devlani and A. K. Rai, *Eur. Phys. J. A* **48**, 104 (2012).
- [12] CDF Collaboration, CDF note 7938 (2005); D0 Collaboration, D0 notes 5026-CONF, 5027-CONF (2006); I. Kravchenko, *arXiv:hep-ex/0605076*.
- [13] T. A. Aaltonen *et al.* (CDF Collaboration), *Phys. Rev. D* **90**, 012013 (2014).
- [14] H. Xu, X. Liu, and T. Matsuki, *Phys. Rev. D* **89**, 097502 (2014).
- [15] Z.-G. Wang, *Eur. Phys. J. Plus* **129**, 186 (2014).
- [16] M. J. Baker *et al.*, *J. High Energy Phys.* **07** (2014) 032.
- [17] S. Narison, *Phys. Lett. B* **718**, 1321 (2013).
- [18] Z.-G. Wang, *J. High Energy Phys.* **10** (2013) 208.
- [19] P. Gelhausen, A. Khodjamirian, A. A. Pivovarov, and D. Rosenthal, *Phys. Rev. D* **88**, 014015 (2013).
- [20] A. Bazavov *et al.*, *Phys. Rev. D* **85**, 114506 (2012).
- [21] H. Na *et al.*, *Proc. Sci.*, LATTICE2012 (2012) 102.
- [22] E. Gamiz, C. T. H. Davies, G. Peter Lepage, J. Shigemitsu, and Matthew Wingate, *Phys. Rev. D* **80**, 014503 (2009).
- [23] Y. Aoki, T. Ishikawa, T. Izubuchi, C. Lehner, and A. Soni (UKQCD Collaboration), *Phys. Rev. D* **91**, 114505 (2015).

- [24] N. H. Christ, J. M. Flynn, T. Izubuchi, T. Kawanai, C. Lehner, A. Soni, R. S. Van de Water, and O. Witzel, *Phys. Rev. D* **91**, 054502 (2015).
- [25] R. J. Dowdall, C. T. H. Davies, T. C. Hammant, and R. R. Horgan (HPQCD Collaboration), *Phys. Rev. D* **86**, 094510 (2012).
- [26] J. Hein, S. Collins, C. T. H. Davies, A. Ali Khan, H. Newton, C. Morningstar, J. Shigemitsu, and J. Sloan, *Phys. Rev. D* **62**, 074503 (2000).
- [27] E. Magyari, *Phys. Lett.* **95B**, 295 (1980).
- [28] M. Shah, B. Patel, and P. C. Vinodkumar, *Phys. Rev. D* **90**, 014009 (2014).
- [29] M. Shah, A. Parmar, and P. C. Vinodkumar, *Phys. Rev. D* **86**, 034015 (2012).
- [30] P. C. Vinodkumar, M. Shah, and B. Patel, Proceedings of the DAE Symp. on Nucl. Phys. **59**, 638 (2014).
- [31] M. Shah, B. Patel, and P. C. Vinodkumar, Proceedings of the DAE Symp. on Nucl. Phys. **59**, 650 (2014).
- [32] M. Shah, B. Patel, and P. C. Vinodkumar, Proceedings of the DAE Symp. on Nucl. Phys. **58**, 626 (2013).
- [33] P. C. Vinodkumar, M. Shah, and B. Patel, *Proc. Sci., HADRON2013* (2013) 078.
- [34] M. Shah, B. Patel, and P. C. Vinodkumar, *Eur. Phys. J. C* **76**, 36 (2016).
- [35] B. Patel and P. C. Vinodkumar, *J. Phys. G* **36**, 035003 (2009).
- [36] A. Parmar, B. Patel, and P. C. Vinodkumar, *Nucl. Phys.* **A848**, 299 (2010).
- [37] A. K. Rai, B. Patel, and P. C. Vinodkumar, *Phys. Rev. C* **78**, 055202 (2008).
- [38] D. Ebert, R. N. Faustov, and V. O. Galkin, *Mod. Phys. Lett. A* **18**, 601 (2003).
- [39] J. P. Lansberg and T. N. Pham, *Phys. Rev. D* **74**, 034001 (2006); **75**, 017501 (2007); *AIP Conf. Proc.* **1038**, 259 (2008).
- [40] C. S. Kim, T. Lee, and G. L. Wang, *Phys. Lett. B* **606**, 323 (2005).
- [41] G. L. Wang, *Phys. Lett. B* **633**, 492 (2006).
- [42] G. Cvetic, C. Kim, G.-L. Wang, and W. Namgung, *Phys. Lett. B* **596**, 84 (2004).
- [43] S. Chatrchyan *et al.* (CMS Collaboration), *Phys. Rev. Lett.* **111**, 101804 (2013).
- [44] R. Aaij *et al.* (LHCb Collaboration), *Phys. Rev. Lett.* **110**, 021801 (2013).
- [45] R. Aaij *et al.* (LHCb Collaboration), *Phys. Rev. Lett.* **111**, 101805 (2013).
- [46] A. J. Buras and R. Fleischer, *Adv. Ser. Dir. High Energy Phys.* **15**, 65 (1998).
- [47] N. Barik, B. K. Dash, and M. Das, *Phys. Rev. D* **31**, 1652 (1985).
- [48] N. Barik and S. N. Jena, *Phys. Rev. D* **26**, 2420 (1982).
- [49] P. C. Vinodkumar, K. B. Vijaya Kumar, and S. B. Khadkikar, *Pramana J. Phys.* **39**, 47 (1992).
- [50] S. B. Khadkikar and K. B. Vijaya Kumar, *Phys. Lett. B* **254**, 320 (1991).
- [51] J. Zeng, J. W. Van Orden, and W. Roberts, *Phys. Rev. D* **52**, 5229 (1995).
- [52] D. Ebert, R. N. Faustov, and V. O. Galkin, *Eur. Phys. J. C* **66**, 197 (2010).
- [53] T. Lahde, C. Nyfalt, and D. Riska, *Nucl. Phys.* **A674**, 141 (2000).
- [54] T. Affolder *et al.* (CDF Collaboration) *Phys. Rev. D* **64**, 072002 (2001).
- [55] E. Eichten, K. Gottfried, T. Kinoshita, K. D. Lane, and T.-M. Yan, *Phys. Rev. D* **17**, 3090 (1978).
- [56] S. F. Radford and W. W. Repko, *Phys. Rev. D* **75**, 074031 (2007).
- [57] N. Brambilla *et al.*, CERN Yellow Report, CERN-2005-05, arXiv:hep-ph/0412158.
- [58] T. A. Lahde, *Nucl. Phys.* **A714**, 183 (2003).
- [59] Q. Ho-Kim and P. Xuan-Yem, *Elementary Particles and Their Interactions: Concepts and Phenomena* (Springer, New York, 1998).
- [60] N. Barik, P. C. Dash, and A. R. Panda, *Phys. Rev. D* **47**, 1001 (1993).
- [61] H. Ciftci and H. Koru, *Int. J. Mod. Phys. E* **09**, 407 (2000).
- [62] K. Hikasa *et al.* (Particle Data Group), *Phys. Rev. D* **45**, S1 (1992).
- [63] J. L. Rosner and S. Stone, arXiv:0802.1043.
- [64] S. Villa, eConf C070512, 014 (2007).
- [65] C. Bobeth, M. Gorbahn, T. Hermann, and M. Misiak, *Phys. Rev. Lett.* **112**, 101801 (2014).
- [66] C. Bobeth, M. Gorbahn, and E. Stamou, *Phys. Rev. D* **89**, 034023 (2014).
- [67] G. Buchalla and A. J. Buras, *Nucl. Phys.* **B400**, 225 (1993).
- [68] A. J. Buras, arXiv:hep-ph/9806471.
- [69] H.-S. Lee, arXiv:1511.03783.
- [70] M. G. Olsson and S. Veseli, *Phys. Rev. D* **51**, 2224 (1995).
- [71] A. Abulencia *et al.*, *Phys. Rev. Lett.* **97**, 062003 (2006).
- [72] A. Abulencia *et al.*, *Phys. Rev. Lett.* **97**, 242003 (2006).
- [73] A. Lenz and U. Nierste, *J. High Energy Phys.* **06** (2007) 072.
- [74] G. Buchalla *et al.*, *Eur. Phys. J. C* **57**, 309 (2008).
- [75] A. J. Buras, W. Slominski, and H. Steger, *Nucl. Phys.* **B245**, 369 (1984).
- [76] T. Inami and C. S. Lim, *Prog. Theor. Phys.* **65**, 297 (1981); **65**, 1772(E) (1981).
- [77] M. Kobayashi and K. Maskawa K, *Prog. Theor. Phys.* **49**, 652 (1973).
- [78] E. Golowich, J. A. Hewett, S. Pakvasa, and A. A. Petrov, *Phys. Rev. D* **76**, 095009 (2007).
- [79] S. Herrlich and U. Nierste, *Nucl. Phys.* **B419**, 292 (1994).
- [80] A. J. Buras, *Phys. Lett. B* **566**, 115 (2003).
- [81] S. N. Jena, H. H. Muni, P. K. Mohapatra, and P. Panda, *Can. J. Phys.* **88**, 517 (2010).
- [82] S. N. Jena, P. Panda, and K. P. Sahu, *J. Phys. G* **27**, 227 (2001).
- [83] H. Ciftci and H. Koru, *Mod. Phys. Lett. A* **16**, 1785 (2001).
- [84] D. Ebert, R. N. Faustova, and V. O. Galkina, *Phys. Lett. B* **537**, 241 (2002).
- [85] M.-Z. Yang, *Eur. Phys. J. C* **72**, 1880 (2012).
- [86] C. W. Hwang, *Phys. Rev. D* **81**, 114024 (2010).
- [87] P. Dimopoulos *et al.*, *J. High Energy Phys.* **01** (2012) 046.